

Nanoscale

Accepted Manuscript



This is an *Accepted Manuscript*, which has been through the Royal Society of Chemistry peer review process and has been accepted for publication.

Accepted Manuscripts are published online shortly after acceptance, before technical editing, formatting and proof reading. Using this free service, authors can make their results available to the community, in citable form, before we publish the edited article. We will replace this *Accepted Manuscript* with the edited and formatted *Advance Article* as soon as it is available.

You can find more information about *Accepted Manuscripts* in the [Information for Authors](#).

Please note that technical editing may introduce minor changes to the text and/or graphics, which may alter content. The journal's standard [Terms & Conditions](#) and the [Ethical guidelines](#) still apply. In no event shall the Royal Society of Chemistry be held responsible for any errors or omissions in this *Accepted Manuscript* or any consequences arising from the use of any information it contains.

: DOI: 10.1039/c0xx00000x

www.rsc.org/xxxxxx

COMMUNICATION

Studying the mechanism of CD47-SIRP α interactions on red blood cells by single molecule force spectroscopyYangang Pan^{a,c}, Feng Wang^a, Yongguang Yang^{b,*} and Hongda Wang^{a,c,*}⁵ Received (in XXX, XXX) Xth XXXXXXXXX 20XX, Accepted Xth XXXXXXXXX 20XX

DOI: 10.1039/b000000x

The interaction forces and binding kinetics between SIRP α and CD47 were investigated by single-molecule force spectroscopy (SMFS) on both fresh and experimentally aged human red blood cells (hRBCs). We found that CD47 experienced a conformation change after oxidation, which influenced the interaction force and the distance of energy barrier between SIRP α and CD47. Our results are significant for understanding the mechanism of phagocytosis of red blood cells at the single molecule level.

Human CD47 consists of an extracellular Ig-like domain, five transmembrane regions with short intervening loops, and a C terminal cytoplasmic tail¹. CD47 functions as an important signaling receptor for the secreted matrix protein thrombospondin-1 and the counter receptor for signal-regulatory protein- α (SIRP α). CD47 can bind to SIRP α on the macrophage and induce inhibitory signaling by the immunoreceptor tyrosine-based inhibition motifs (ITIMs) residing in the cytoplasmic tail of SIRP α ^{2,3}. Studies have proved that CD47 was often termed a “don’t-eat-me” signal through its effect on SIRP α ^{4,5}. However, recent work has shown that binding CD47 to SIRP α can also yield an “eat me” signal for old hRBCs phagocytosis⁶. Although

it has been shown that CD47 expression is reduced on aged RBCs^{7,8}, other reports imply that CD47 levels remain invariant^{9,10}. In addition, CD47 on hRBCs that had been stored for prolonged time probably underwent a conformational change⁶. All these findings suggest that the CD47 alteration might switch CD47-SIRP α signalling on hRBCs. So far, how the change of CD47-SIRP α interactions in aged RBCs affects phagocytosis remain unclear.

Due to the high sensitivity of the atomic force microscopy cantilever, single molecule force spectroscopy (SMFS) is considered as a power tool for measuring the binding forces between biomolecules and coordinative bonding forces in transition metal complex¹¹⁻¹⁹. Here, we used force spectroscopy to investigate whether and how the change of CD47 molecule in experimentally aged RBCs affects its binding to SIRP α .

SMFS was carried out to detect the interaction force between SIRP α and CD47 on both fresh and experimentally aged hRBCs. For this purpose, the SIRP α proteins were covalently conjugated onto an AFM tip via a heterobifunctional PEG-NHS linker and the force distance cycle was engaged on the RBCs membranes. Figure 1a shows the tip chemistry. The PEG linker was immobilized on the aminated AFM probe through the NHS terminus. The surface density of molecules was regulated so that single molecule could be detected²⁰. The SIRP α were covalently conjugated with the PEG linker through forming schiff base between the cysteine and the aldehyde group at the free end of the cross-linker. From the bright-field image of AFM tip, we could locate the pyramid shaped probe. By the fluorescence imaging, we observed fluorescence spots on the apex of the AFM tip, confirming that Cy5-labeled SIRP α were successfully attached on the AFM tip, as illustrated in Figure 1b. To explore the mechanism of controlling the phagocytosis through the interaction of CD47-SIRP α , force-distance curves were performed by the SIRP α -functionalized tip on both fresh and aged hRBCs. Bright-field images of fresh and aged hRBCs are illustrated in Figure 1c and Figure 1d. After oxidation, the membranes of hRBCs were wrinkled.

^aState Key Laboratory of Electroanalytical Chemistry, Changchun Institute of Applied Chemistry, Chinese Academy of Sciences, Changchun, Jilin 130022, P.R. China.

^bInstitute of Immunology, The First Bethune Hospital Academy of Translational Medicine, Jilin University, Changchun, 130012, China

^cUniversity of Chinese Academy of Sciences, Beijing 100049, P.R. China.

† Electronic Supplementary Information (ESI) available: Experimental section. See DOI: 10.1039/b000000x/

* Corresponding author: hawang@ciac.ac.cn, yongguang.yang@gmail.com.

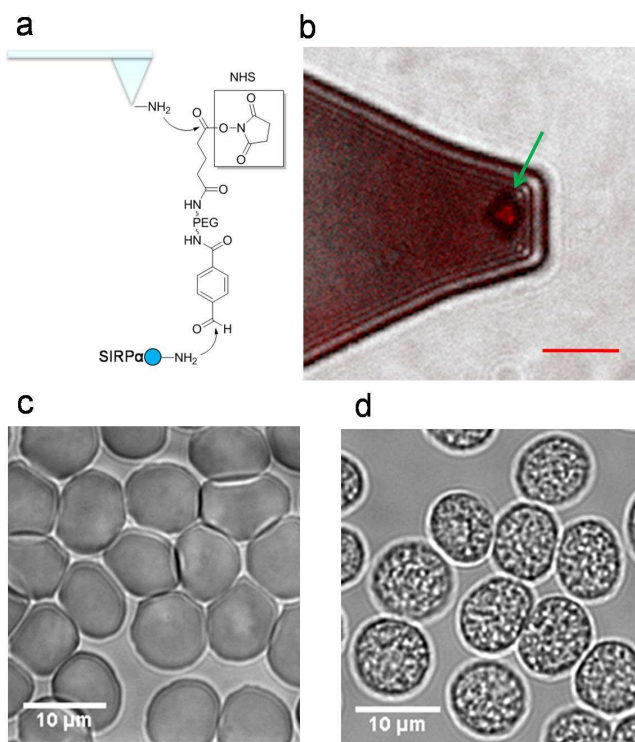


Figure 1. The tip chemistry. (a) Scheme of SIRPα conjugation to the AFM tip via a heterobifunctional PEG linker. (b) Fluorescent image of AFM tip modified with SIRPα. The arrow indicates that SIRPα was successfully attached on the apex of AFM tip. (c) Bright-field image of fresh hRBCs. (d) Bright-field image of experimentally aged hRBCs. Scale bars: 10 μm in (b), (c) and (d) respectively.

Figure 2a shows a typical force-distance curve recording the interactions between SIRPα and CD47 on fresh hRBCs. Before

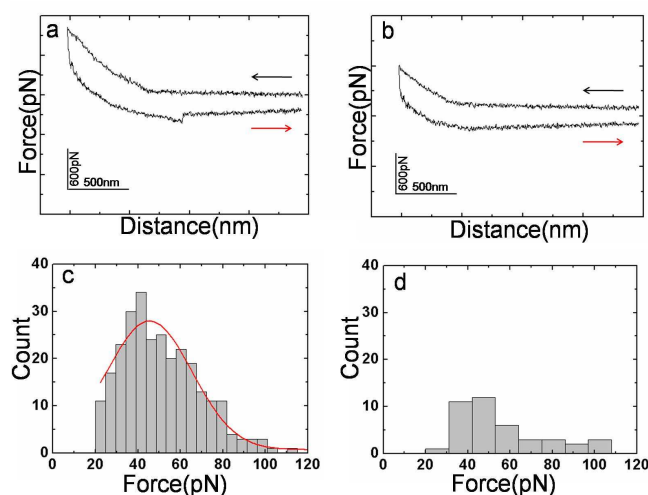


Figure 2. The force measurement on fresh hRBCs. (a) A typical force-distance curve between SIRPα and CD47. (b) A typical force-distance curve after blocking with free SIRPα. (c) The distribution of unbinding force between SIRPα and CD47 on fresh hRBCs ($n > 270$ that were chosen randomly from about 1300 force curves). (d) The histogram of unbinding probability after blocking (unbinding probability is about 2.1%).

the AFM tip modified with SIRPα touched with hRBCs, the right part of the force curve was horizontal (top line). As the AFM tip approached and then interacted with the hRBCs membranes, a gentle slope appeared during the tip pressing on them, which is the feature of engaging the force curve on soft living cells²¹. A SIRPα/CD47 complex would be formed during the contact period. Subsequently, the interaction force between the SIRPα and CD47 on hRBCs membranes could be detected during the following retraced process in which the distance between the AFM tip tethered with SIRPα and the cell membrane was increasing (low line). The SIRPα and CD47 complex would finally break at a critical point, and the tip jumped back to the rest position. Figure 2b shows the typical force-distance curve after blocking with CD47 antibody. The force can be calculated from the deflection signal that occurred at the broken point. The force we detected was about 50 ± 18 pN at a retraction velocity of $4 \mu\text{m s}^{-1}$, as illustrated in Figure 2c. To prove that the measured force signals were indeed a consequence of the SIRPα-CD47 interaction, CD47 antibody was injected into the working chamber. We found that most of force signals disappeared in the force curves, as shown in Figure 2d.

Figure 3a represents a typical force-distance curve recording the force interactions between SIRPα and CD47 on aged hRBCs. The force is about 151 ± 53 pN at a retraction velocity of $4 \mu\text{m s}^{-1}$, as

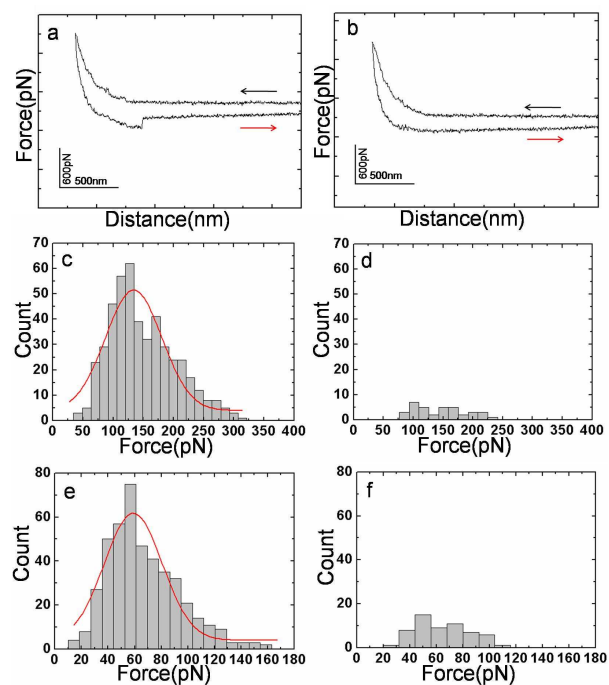


Figure 3. The force measurement on experimentally aged hRBCs. (a) A typical force-distance curve between SIRPα and CD47. (b) A typical force-distance curve after blocking with free SIRPα. (c) The distribution of unbinding force between SIRPα and CD47 on experimentally aged hRBCs ($n > 400$, chosen randomly from about 2000 force curves). (d) The histogram of unbinding probability after blocking. (e) The distribution of unbinding force between SIRPα and CD47 on experimentally aged hRBCs that had been incubated with free cysteine ($n > 400$, chosen randomly from about 2000 force curves). (f) The histogram of unbinding probability after blocking.

shown in Figure 3b. After blocking with CD47 antibody, unbinding probability was obviously decreased from 23.4% to 1.8% (Figure 3b and 3d). We also experimentally aged the hRBCs that had been incubated with free cysteine, and then we performed the force-distance curves on these hRBCs. The most probable unbinding force values were about 62.1 ± 21.3 pN at a retraction velocity of $4 \mu\text{m s}^{-1}$, as illustrated in Figure 3e. After blocking with CD47 antibody, unbinding probability obviously decreased from 25.5% to 2.9%, which confirms that the binding signals were from the specific interactions of CD47/SIRP α .

To obtain the distance of the energy barrier, we performed the force distance curves at various pulling velocities. The rupture of weak bonds under a force is related to the loading rate, and the bond rupture will occur more easily at lower loading rate²². By fitting the plot in Figure 4 to Eq. 1 (Materials and Methods), we can extract the distance of energy barrier x_β . The plots of unbinding forces vs. loading rates were displayed in Figure 4. It can be calculated that on fresh hRBCs, $x_\beta = 0.97$ nm; on aged hRBCs, $x_\beta = 0.16$ nm. When we experimentally aged the hRBCs incubated with free cysteine, x_β on these hRBCs is about 0.59 nm.

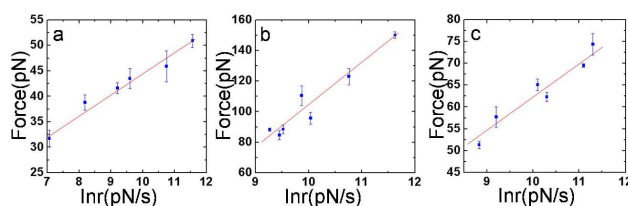


Figure 4. Loading rate dependence of unbinding force of SIRP α /CD47 on fresh hRBCs(a), experimentally aged hRBCs (b), experimentally aged hRBCs incubated with free cysteine (c), respectively.

The extracellular Ig-like domain of CD47 is required for the interaction between CD47 and SIRP α ²³. As illustrated in Figure 5, the Ig-like domain on fresh hRBCs contains a residue Cys-15 and the membrane-spanning (MMS) domain of CD47 including two residues Cys-241 and Cys-245, which is same as a structural model made by previous report¹. The cysteine residues (Cys-SH) in protein mostly remain protonated at physiological pH; thus the residues Cys in cytoplasmic proteins may not form disulfide bonds²⁴. Our data show that the probable unbinding forces between SIRP α and CD47 on aged hRBCs are much larger than those on fresh hRBCs (Figure 3c and Figure 2c). In addition, the dynamic force data verified that the distance x_β for SIRP α /CD47 on experimentally aged hRBCs is shorter than that on fresh hRBCs. Because the local structure near the mechanical “breakpoint”²⁵ (bond between CD47 and SIRP α) can strongly influence the unbinding force (the stiffer domains with shorter distances to their transition states maintain their structure to higher applied forces²⁵⁻²⁷), our results imply that CD47 underwent the conformational change after oxidation. Recent work suggests that oxidative stress promotes disulfide bond formation within families of cytoplasmic proteins and may provide a common mechanism used to control multiple physiological processes²⁸. Therefore, we assumed that free Cys-15 might form disulfide bond with Cys-241 or Cys-245 after oxidation, as illustrated in Figure 5. To support this hypothesis, we have aged the hRBCs incubated with free cysteine, and found

that the probable unbinding forces between SIRP α and CD47 on these hRBCs were similar to those on fresh hRBCs (Figure 3e and Figure 2c), as the disulfide bonds prefer to be formed between Cys residue and free cysteine rather than between Cys residues (free cysteine blocked the formation of disulfide bonds between residues).

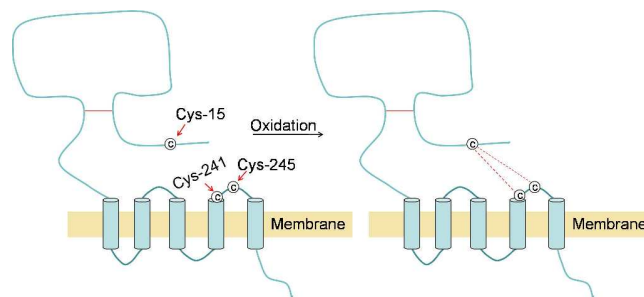


Figure 5. The scheme of CD47 structure on the membrane before (left) and after (right) oxidation.

Conclusion

We demonstrate that the interactions between SIRP α and CD47 on aged hRBCs were more stable than that on fresh hRBCs, and the residue Cys-15 in Ig-like domain could form disulfide bond with Cys-241 or Cys-245 in MMS domain after oxidation, revealing that the conformational change of CD47 affects its interaction with SIRP α . Our results may provide an insight in the mechanism of CD47-SIRP α signalling switch on red blood cells.

Acknowledgement

This work was financially supported MOST (Grant No. 2011CB933600 to HW, Grant No. 2013CB966900 to YY), NSFC (Grant No. 21373200 to HW, Grant No. 81273334 to YY), and Program for Changjiang Scholars and Innovative Research Team in University (PCSIRT, IRT1133).

Notes and references

- 1 F. P. Lindberg, H. D. Gresham, E. Schwarz and E. J. Brown, *J Cell Biol*, 1993, **123**, 485-496.
- 2 T. Matozaki, Y. Murata, H. Okazawa and H. Ohnishi, *Trends Cell Biol*, 2009, **19**, 72-80.
- 3 R. Sato, H. Ohnishi, H. Kobayashi, D. Kiuchi, A. Hayashi, Y. Kaneko, N. Honma, H. Okazawa, Y. Hirata and T. Matozaki, *Biochem. Biophys. Res. Commun.*, 2003, **309**, 584-590.
- 4 A. N. Barclay and M. H. Brown, *Nat. Rev. Immunol.*, 2006, **6**, 457-464.
- 5 T. K. van den Berg and C. E. van der Schoot, *Trends Immunol.*, 2008, **29**, 203-206.
- 6 P. Burger, P. Hilarius-Stokman, D. de Korte, T. K. van den Berg and R. van Bruggen, *Blood*, 2012, **119**, 5512-5521.
- 7 L. Fossati-Jimack, S. A. da Silveira, T. Moll, T. Kina, F. A. Kuypers, P. A. Oldenburg, L. Reininger and S. Izui, *J. Autoimmun.*, 2002, **18**, 17-25.
- 8 S. Khandelwal, N. van Rooijen and R. K. Saxena, *Transfusion*, 2007, **47**, 1725-1732.
- 9 A. Stewart, S. Urbaniak, M. Turner and H. Bessos, *Transfusion*, 2005, **45**, 1496-1503.
- 10 A. M. Annis and R. L. Sparrow, *Transfus. Apher. Sci.*, 2002, **27**, 233-238.
- 11 Y. Shan, J. Huang, J. Tan, G. Gao, S. Liu, H. Wang and Y. Chen, *Nanoscale*, 2012, **4**, 1283-1286.

- 12 R. Zhu, S. Howorka, J. Proll, F. Kienberger, J. Preiner, J. Hesse, A. Ebner, V. P. Pastushenko, H. J. Gruber and P. Hinterdorfer, *Nat Nano*, 2010, **5**, 788-791.
- 13 L. Wildling, C. Rankl, T. Haselgrübler, H. J. Gruber, M. Holy, A. H. Newman, M.-F. Zou, R. Zhu, M. Freissmuth, H. H. Sitte and P. Hinterdorfer, *J. Biol. Chem.*, 2012, **287**, 105-113.
- 14 P. Hinterdorfer, W. Baumgartner, H. J. Gruber, K. Schilcher and H. Schindler, *Proc. Natl. Acad. Sci. U. S. A.*, 1996, **93**, 3477-3481.
- 15 E. L. Florin, V. T. Moy and H. E. Gaub, *Science*, 1994, **264**, 415-417.
- 16 Y. Shan, S. Ma, L. Nie, X. Shang, X. Hao, Z. Tang and H. Wang, *Chem Commun*, 2011, **47**, 8091-8093.
- 17 W. Zhao, M. Cai, H. Xu, J. Jiang and H. Wang, *Nanoscale*, 2013, **5**, 3226-3229.
- 18 M. Zhang, B. Wang and B. Xu, *Phys Chem Chem Phys*, 2013, **15**, 6508-6515.
- 19 X. Hao, N. Zhu, T. Gschneidner, E. O. Jonsson, J. Zhang, K. Moth-Poulsen, H. Wang, K. S. Thygesen, K. W. Jacobsen, J. Ulstrup and Q. Chi, *Nat Commun*, 2013, **4**.
- 20 C. K. Riener, F. Kienberger, C. D. Hahn, G. M. Buchinger, I. O. C. Egwim, T. Haselgrubler, A. Ebner, C. Romanin, C. Klampfl, B. Lackner, H. Prinz, D. Blaas, P. Hinterdorfer and H. J. Gruber, *Anal. Chim. Acta*, 2003, **497**, 101-114.
- 21 Y. Shen, J. L. Sun, A. Zhang, J. Hu and L. X. Xu, *Phy. Med. Biol.*, 2007, **52**, 2185-2196.
- 22 E. Evans and K. Ritchie, *Biophys. J.*, 1997, **72**, 1541-1555.
- 23 E. J. Brown and W. A. Frazier, *Trends Cell Biol.*, 2001, **11**, 130-135.
- 24 A. Rietsch and J. Beckwith, *Annu. rev. genet.*, 1998, **32**, 163-184.
- 25 C. Bustamante, Y. R. Chemla, N. R. Forde and D. Izhaky, *Annu. Rev. Biochem.*, 2004, **73**, 705-748.
- 26 H. Li, W. A. Linke, A. F. Oberhauser, M. Carrion-Vazquez, J. G. Kerkvliet, H. Lu, P. E. Marszalek and J. M. Fernandez, *Nature*, 2002, **418**, 998-1002.
- 27 A. F. Oberhauser, C. Badilla-Fernandez, M. Carrion-Vazquez and J. M. Fernandez, *J. mol. biol.*, 2002, **319**, 433-447.
- 28 S. Finke and K. K. Conzelmann, *Virus Research*, 2005, **111**, 120-131.